Essential Readings in Light Metals: Cast Shop for Aluminum Production.
Edited by John F. Grandfield and Dmitry G. Eskin.
© 2013 The Minerals, Metals & Materials Society. Published 2013 by John Wiley & Sons, Inc.

STUDIES OF THE ACTION OF GRAIN-REFINING PARTICLES IN ALUMINIUM ALLOYS

P. Schumacher and A.L. Greer
University of Cambridge,
Department of Materials Science and Metallurgy,
Pembroke Street, Cambridge CB2 3QZ (UK).

Abstract

Crystallization from a melt and from a metallic glass both occur in an undercooled liquid. In this way identical nucleation mechanisms can operate in the two cases. However, in metallic glasses, unlike conventional solidification at low undercooling, the low atomic mobility permits the resolution and microscopical study of nucleation processes on added particles. Conventional aluminium grain-refiner based on Al-Ti-B has been used to obtain nucleant particles embedded in a glassy matrix of $Al_{85}Y_8Ni_5Co_2$ (at%). During crystallization from the glassy state, nucleation and growth of α-Al can be observed on TiB_2 particles coated with a layer of Al_3Ti. Empirical relations found in casting practice of Al-alloys, such as excess Ti necessary for grain refinement, can be related to the observed nucleation mechanism, which is found to be very sensitive to both crystallographic and chemical factors.

Introduction

In aluminium alloys, grain refinement is achieved by the addition of a grain-refiner rod, based typically on the Al-Ti-B alloy system. The rod contains Al_3Ti and TiB_2 particles embedded in an Al matrix and a standard composition is Al – 5 wt.% Ti – 1 wt.% B). Growth of primary Al nuclei occurs only on some of the added particles during casting and the role of these sites during the nucleation process and their actual nucleation mechanism is not well understood. Furthermore the nucleation process can be influenced by solute elements, (e.g. Zr apparently poisons grain refinement [1]), and can be time-dependent (e.g. when the refiner is contact with the melt for long times, fading of the refiner efficiency occurs [2]). There is a peritectic reaction (liquid + $Al_3Ti \rightarrow$ α-Al) at 3°C above the melting point of pure aluminium. This reaction is believed to be a powerful nucleation mechanism yielding α-Al [3] when a stable substrate is available for heterogeneous nucleation. However, under typical melting and casting conditions (750°C for 10 min), grain refinement can be observed in very dilute aluminium alloys (0.03- 0.08 wt% Ti) well beyond expected dissolution times for Al_3Ti particles [4]. While boride particles are expected to be stable even in dilute aluminium melts, it was found empirically [5] that their grain-refining performance is greatly reduced when no excess Ti, i.e. Ti beyond stoichiometric TiB_2, is present. So far the role of the excess Ti remains unclear, but it has been supposed that excess Ti in the form of Al_3Ti, is somehow preserved even in dilute melts by the addition of the TiB_2 particles. That is, the grain refining is due to a combined action of Al_3Ti and TiB_2. Various suggestions have been made about how the TiB_2 could act to preserve the Al_3Ti locally, through:

1. a surrounding shell of borides [6,7];
2. a survival in cavities [8];
3. an adsorption layer on borides [9].

The key to successful formation of α-Al on substrates by the suggested mechanisms is their crystallographic matching [10] and/or their chemical composition at the nucleating interface [3]. However, investigation of the mechanisms proposed above is difficult since it is not possible to observe directly the actual nucleation mechanism in dilute aluminium alloys. Any microstructural investigation in dilute aluminium alloys is hindered by the high atomic mobility and non-

isothermal casting conditions. Indirect observations of the as-cast microstructure often remain inconclusive since the microstructure depends not only on nucleation but also on subsequent growth.

While there is some debate over the correct description of critical nuclei during the liquid to solid transformation [11], it appears that the same physical mechanism of stochastic cluster fluctuation is valid for nucleation from a glass and from a melt. Both transformations – crystallization from the glass (devitrification) and crystallization from the melt (solidification) – occur in an undercooled liquid. The undercoolings achieved are much larger in the case of devitrification and hence the driving forces for nucleation and growth are also larger. The rate-limiting process in devitrification is atomic transfer across the interface or solute transport, while in solidification it is predominantly heat flow. However, the important point in this comparison is the difference in the atomic mobility estimated, which is inversely related to the viscosity of the liquid. In crystallization from the glass the atomic mobility is slower than crystallization from the melt at low undercooling by a factor of approximately 10^{16}. The similarities and contrasts between devitrification and conventional solidification are summarized in Table I. In the present work, the similarities are such that crystallization of α-Al from an Al-based metallic glass can be regarded straightforwardly as a slow motion analogue of the solidification of a dilute aluminium melt. This analogy is exploited here to study nucleation on conventional grain-refining particles.

Aluminium-based metallic glasses can be made by rapid quenching of the melt. In the present work, melt-spinning ($\dot{T} \approx 10^5 - 10^6$ K s^{-1}) is used. A suitable glass for the study of nucleation on grain refining particles has to fulfil various conditions [12]. The composition has to have sufficient glass-forming ability such that after melt-spinning only negligible crystalline volumes can be found on added nucleation sites; it has to show α-Al during devitrification, and the nucleation density in the glass matrix has to be sufficiently low in order to distinguish between nucleation on added sites and nucleation in the matrix which is unaffected by added sites. The observation of nucleation events is favoured by a slow growth rate and a time delay between the nucleation onset on added sites and nucleation in the matrix, so that impingement of crystal growth from different nucleation events can be avoided. Previous work [13,14] has shown that amorphous $Al_{85}Y_8Ni_5Co_2$ (at.%) (which is known to be relatively stable [15,16]) can be used to study the action of commercial grain-refiner additions. In this work it will be shown how holding times (of refiner in the high-temperature melt before quenching) can affect the nucleation mechanism for α-Al.

Table I Comparison between crystallization from the glass and from the melt

	Crystallization from the glass (devitrification)	Crystallization from the melt (solidification)
composition range	90 – 75 at.% Al	100 – 99.9 at.% Al
initial state	very viscous, essentially solid	fluid
relative melt undercooling $\Delta T/T_m$	~ 0.5	~ 0.01
rate-limiting step	solute transport or interfacial kinetics	heat flow
normalized atomic mobility	10^{-16}	1
driving force for nucleation	large	small
crystallizing phases	≥1	1

Experimental methods

Various alloys for melt-spinning were prepared *in situ* in a melt-spinning crucible (BN) from conventional aluminium grain-refiner rods (London & Scandinavian Metallurgical Co.) and a master alloy prepared by arc melting on a copper hearth under inert (argon) atmosphere from aluminium (99.999%), yttrium (99.9%), nickel (99.99%) and cobalt (99.99%). In the grain-refiner rod and in the final alloy, the boron is expected to be entirely in TiB_2 particles, leaving any

excess Ti dissolved in the matrix. The solute content of the master alloy was selected so that the matrix composition of the alloys studied here matches as closely as possible the $Al_{85}Y_8Ni_5Co_2$ used in an earlier devitrification study [12,16] without added particles. Ribbons were prepared with added grain-refiner rod of the well known composition Al – 5 wt.%Ti – 1 wt.%B. Thus the final overall compositions (at.%) of the ribbons were :

$$\{Al_{85}[Y_8Ni_5Co_2]_{15-x} + (\text{excess Ti})_x\}_{100-y} + \{TiB_2\}_y$$

with $x = 0.10$ and $y = 0.32$. Approximately 5 wt.% of the aluminium content of the matrix comes from the grain-refiner rod. The melt-spinning was carried out in inert atmosphere (helium) with a surface wheel speed of 40 m s^{-1}. The melt was held at 1300°C (measured with a two-colour pyrometer with closed-loop control of the radio-frequency heating unit) for 0, 1, 3, 6, 12, 24, 48 min before ejection. Typical melt-spun ribbon dimensions were 30 μm × 2 mm. Samples for transmission electron microscopy (TEM) were prepared by electropolishing using 4% perchloric acid in ethanol at –25° C. Energy-dispersive X-ray (EDX) analysis was used with a Philips 400 microscope.

Results and Discussion

Microstructure of the as-quenched samples

In the as-quenched state particles can be observed (figure 1) within the melt-spun ribbons. The particles are not uniformly distributed and appear in bands along the melt-spinning direction. The particles exhibit facets and have a hexagonal structure; electron diffraction indicates c/a-ratios of 1.01 to 1.06, close to the values for AlB_2 (1.083) and TiB_2 (1.066). In earlier work [13] boron was detected in these particles in thin areas of TEM samples using a microprobe. These particles could correspond to the $(Ti_{1-x}Al_x)B_2$ phase reported in grain-refining master alloys by Johnson and Bäckerud [17]. No separate Al_3Ti particles were found in the samples, thus indicating total dissolution of separate aluminide particles at the comparatively high melt temperature prior to ejection for melt-spinning.

To observe nucleation events, the thin foils were tilted to have the electron beam direction parallel or perpendicular to facets of boride particles, i.e. parallel

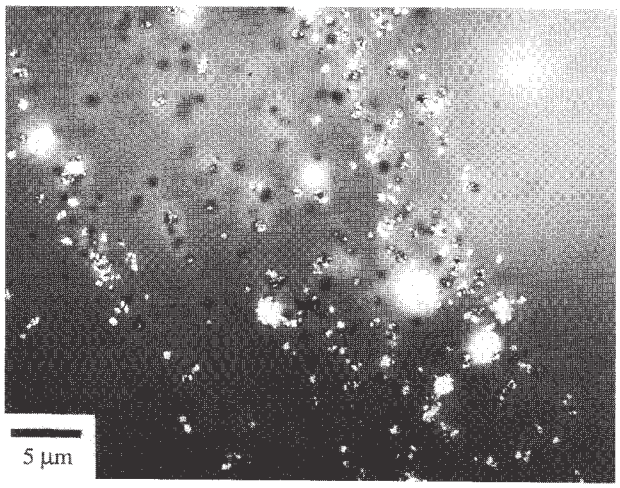

Figure 1:
Boride particles in a glassy matrix ($Al_{85}Y_8Ni_5Co_2$ + excess Ti) obtained by melt-spinning: bright-field TEM micrographs of the as-quenched state. The particles are non-uniformly dispersed, appearing in bands along the melt-spinning direction.

to the <1010>, <11$\bar{2}$0>, or <0001> zone axes of the hexagonal boride phase. In figure 2, a boride particle can be seen for which the electron beam is parallel to the <11$\bar{2}$0> zone axis. The melt was held at 1300°C for 1 min before quenching and the micrograph shows the as-quenched state of the sample. In bright-field (figure 2a) it can be seen that α-Al has nucleated and grown on the {0001} faces of the boride (which has been preferentially etched). This indicates that despite the high cooling rates (10^6 K s^{-1}) the {0001}faces of the boride are heterogeneous sites of sufficient potency to permit nucleation of α-Al during the quench. The aluminium becomes more clearly visible in dark-field (figure 2c) with the objective aperture on the {111}Al spot. Many Al crystals have been nucleated on the basal face of the boride, consistent with their growth being sufficiently slow to permit further nucleation events rather than rapid coverage of the boride by growth from a single event, as might be expected for nucleation at low undercooling. The existence of many α-Al crystals in non-random orientation (as shown by the dark-field micrograph) demonstrates that there is an epitaxial relationship between the α-Al and the TiB_2. In figure 2b the faceted nature of the boride is illustrated by dark-field imaging with the objective aperture on the {0001}TiB_2 spot. There are some ledges on the boride, but consistent with earlier work [14] it appears that α-Al does not nucleate

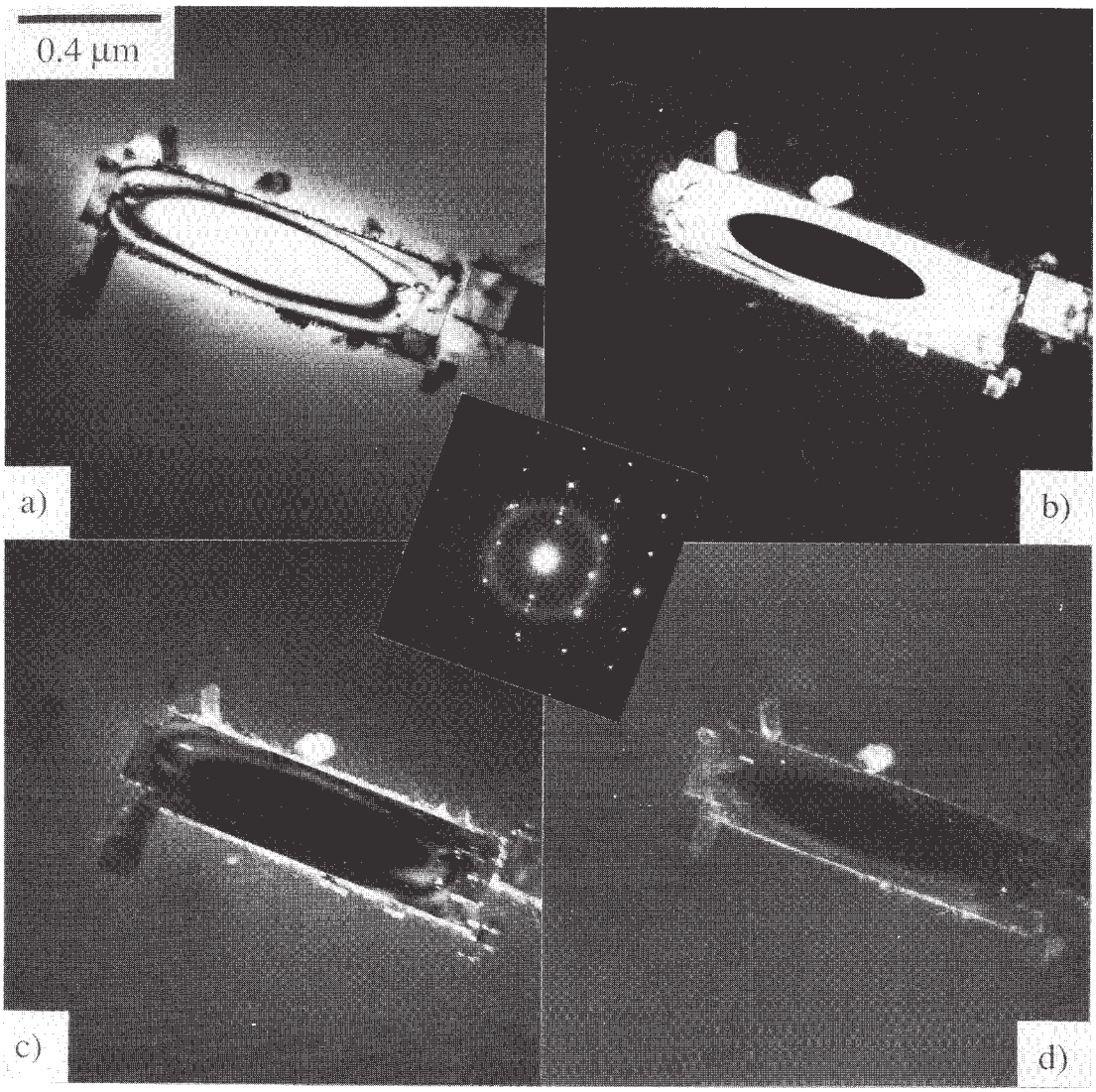

Figure 2:
TEM micrographs of a boride particle in an as-quenched glassy sample. The melt was held at 1300°C for 1 min before quenching. The electron beam is parallel to <11$\bar{2}$0> of the boride. Bright-field a), and dark-field with the objective aperture b) on the {0001}TiB_2 spot, c) on the {111}Al spot and d) on the {112}Al_3Ti spot. There is a layer of Al_3Ti on the boride, and α-Al has nucleated on this layer only on the basal faces of the boride. Inset: corresponding selected area diffraction pattern.

preferentially in the corners formed by the ledges but on {0001} boride faces. Interestingly, electron diffraction (pattern inset in figure 2), shows that in the <11$\bar{2}$0>TiB_2 pattern, there are three spots aligned in the <0001>TiB_2 direction. These correspond to the {111}Al, the {0001}TiB_2 and a third phase which can be illuminated in dark-field with the objective aperture on that third spot (figure 2d). The third phase is highlighted as a thin layer in figure 2d and indeed some streaking can be detected in its diffraction maxima (inset figure 2).

Orientation relationship

Selected area diffraction patterns from the rim of the particles reveal two types of pattern (figure 3). In both types the <110>Al pattern is aligned with the dominant <11$\bar{2}$0>TiB_2 pattern, the close-packed planes being parallel: {111}Al ∥ {0001}TiB_2. Between the {111}Al and {0001}TiB_2 reflections a third spot, corresponding to the layer, can be found. Consistent with earlier work [12,13,14,18] this layer has been identified as Al_3Ti. A similar orientation relationship between Al

and the boride, but without detection of any layer has been found in rapidly quenched refiner alloys [19]. In tetragonal Al_3Ti the {112} planes can be termed pseudo-close-packed because the c/a ratio (c/a = 2.23) is close to 2. The {112}Al_3Ti planes are parallel to the close-packed planes of the boride and Al. The close-packed directions in the three phases also appear to be parallel. Because of the lower symmetry of the Al_3Ti, there are two orientation relationships as indicated in Table II. Each relationship has a number of crystallographically equivalent but distinguishable variants. Furthermore, some misorientation between the close-packed planes has been observed. By tilting to the $<11\bar{2}0>$ zone axis of TiB_2 in most cases the diffraction maxima indicate aligned {111}Al, {112}Al_3Ti and {0001}TiB_2 planes. Both orientation relationships in Table II can be observed, even simultaneously, though 2 is more common. However, it is difficult to distinguish between the <110>Al and <210>Al_3Ti patterns (see figure 3b). It is interesting to note that the presence of Al_3Ti as a thin layer on the basal plane of the boride exposes a non-equilibrium facet {112}Al_3Ti to the liquid rather than the equilibrium facets {110} and {001}Al_3Ti described by Arnberg, Bäckerud and Klang [20]. The {112} faces on Al_3Ti must have a relatively high interfacial energy with liquid Al. Furthermore, they have been reported to have a good semi-coherent crystallographic matching to the {111}Al planes [21]. For these reasons the thin layer of Al_3Ti on the boride may be an even better nucleant for α-Al than isolated Al_3Ti particles.

Table II Orientation relationships between Al, Al_3Ti and TiB_2.

No.	TiB_2	Al_3Ti	Al
1	$<11\bar{2}0>\{0001\}$	<110>{112}	<110>{111}
2	$<11\bar{2}0>\{0001\}$	<210>{112}	<110>{111}

Effects of holding time

Holding of the samples in the liquid state at 1300°C for up to 48 min prior to quenching does not result in dissolution of the boride particles. It should be noted that there is no settling of boride particles in the melt (as can be observed in conventional casting systems) because the radio frequency heating induces vigorous

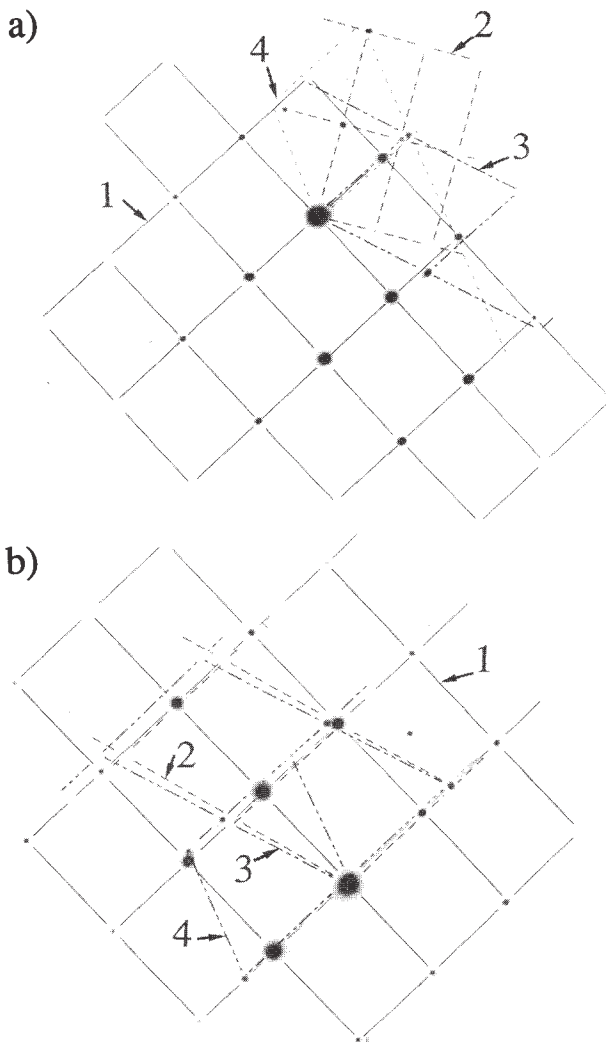

Figure 3:
Typical selected area diffraction patterns from boride particles nucleating α-Al, with the electron beam parallel to the $<11\bar{2}0>TiB_2$ zone axis. These patterns are superimposed with the close-packed planes in each phase aligned. The patterns are in a) the $<11\bar{2}0>TiB_2$ (1), <110>Al_3Ti (2) and <110>Al (3) and in b) the $<11\bar{2}0>TiB_2$ (1), <210>Al_3Ti (2) and <110>Al (3).

stirring of the melt. After holding for 6 min at 1300°C prior to quenching the as-quenched ribbon shows boride particles with increased layer thickness of the Al_3Ti as illustrated in figure 4. That the aluminide layer has been formed in the melt is consistent with previous work [13]. For various holding times in the melt (at 1300°C) the data in figure 5 show that the layer thickness increases rapidly at first and then appears to saturate. The driving force for growth of the layer remains unclear. From the binary Al-Ti phase diagram

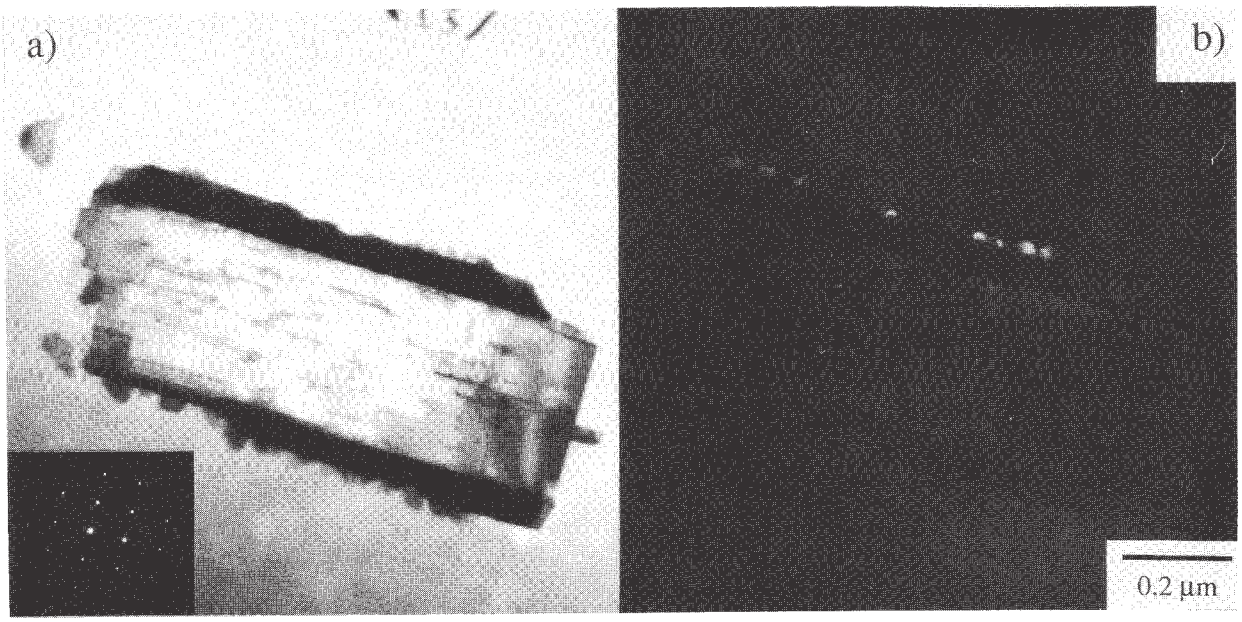

Figure 4:
Bright-field TEM micrographs of a boride particle in an as-quenched glassy sample. The melt was held at 1300°C for 6 min before quenching. The electron beam is parallel to <11$\bar{2}$0> of the boride. In comparison with figure 2 it is clear that with increased holding time the aluminide layer grows considerably and develops facets. α-Al can be observed on the aluminide layer in dark-field TEM with the objective aperture on the {111}Al spot.

no aluminide layer is expected but such a layer might be stabilized by adsorption effects at the boride-aluminide interface. This could explain a thin layer of aluminide on the boride but not its growth. However, adsorbed traces of tantalum have been found in the layer by EDX-mapping in previous work [13] and in the present work by EDX-spot analysis. Tantalum is an impurity element in the yttrium which has been used as a component of the glassy matrix. There is perfect solid solubility of the isomorphous phases Al_3Ti and Al_3Ta which both exhibit a peritectic reaction with an Al-rich melt. Although there are no data on the phase diagram of the multi-component system used in this study, it could be possible that the combined content of Ti and Ta causes a shift of the composition so that an $Al_3(Ti,Ta)$ phase is stable in the Al-rich liquid/glass. Hence, in the initial stages the layer can grow until equilibrium is achieved as indicated in figure 5. On the other hand it is not clear how the growth of the layer affects the efficacy of nucleation on the layer. It appears that at longer holding time the aluminide layer itself forms facets such as those visible in figure 4. The new facets are of the type reported by Arnberg et al. [20]. So far it remains unclear if the new faces have a different nucleation potency from the {112} faces of the thin layer. Recent investigations [22] of added

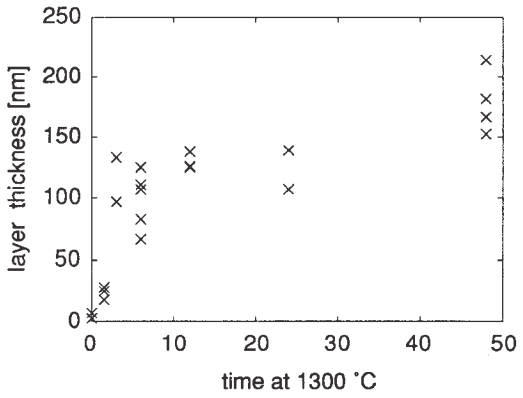

Figure 5:
Thickness of the aluminide layer found on the boride particles in the as-quenched state as a function of the melt holding time at 1300°C prior to quenching. The layer grows rapidly for short annealing times.

boride particles and excess Ti in conventional Al melts have shown that boride particles can nucleate Al_3Ti and are located inside Al grains. In agreement with the present work it is suggested that the aluminide has nucleated α-Al. The micrographs in [22] show plate-like aluminide crystals which may exhibit facets with similar orientation to the faceted aluminide observed in the present study after long holding times.

Discussion

It is important to establish whether it is valid to interpret the nucleation events observed on grain-refining particles in the present study as a slow-motion analogue of the processes in conventional solidification. The phenomena observed in the glassy matrix show several similarities with those found in conventional processing. In both cases:

— Al_3Ti particles present in the refiner rod dissolve in the melt consistent with their reported short survival times [3,4].
— TiB_2 particles survive and act as centres from which α-Al grows.
— The peritectic reaction remains possible because Al_3Ti is preserved in association with boride particles, even after the dissolution of separate Al_3Ti particles;
— Excess Ti is necessary for effective nucleation of α-Al [5,18].
— Nucleation of α-Al occurs on a semi-coherent interface ({112}Al_3Ti face) which has been predicted as a good nucleation substrate [21].
— The orientation relationship (across Al_3Ti) is $\{0001\}TiB_2 \parallel \{111\}Al$ and $<11\bar{2}0>TiB_2 \parallel <110>Al$ [19].
— In the presence of sufficient excess Ti (or of another element promoting formation of a phase isomorphous with Al_3Ti), the Al_3Ti phase grows from boride particles and develops {110} and {001} facets [20,22].
— No fading by dissolution of the Al_3Ti has been observed and fading appears to be related to settling of borides with an active Al_3Ti layer [2].

The Al_3Ti layer on the boride particles found in the present work has not been observed in grain-refined dilute Al alloys or in rapidly quenched refiner rod with excess Ti [19]. However, the strong similarities in the effect of excess Ti on nucleation suggest that further detailed microstructural studies on conventional material would be worthwhile.

There are clear differences between the glass in the present work and a dilute aluminium melt:

— The glass is chemically different, with higher solute content.
— The effective undercooling is much greater in the glass than in the conventional case.

Notwithstanding the higher solute content in the glass, no extra phases were found in the present work, either present initially or forming by reaction. The role of Ta impurity in promoting growth of the $Al_3(Ti,Ta)$ layer is an unwanted effect of the different composition, but can be removed in future work. If extra solute elements dissolve either in the TiB_2 or in the α-Al, the lattice parameters and crystallographic matching could be altered.

The large undercooling in the metallic glass should increase the likelihood of nucleation even on heterogeneous sites of limited potency. The different temperatures in the present work and in the conventional case could, because of differential thermal expansion alter crystallographic matching. The effect of undercooling in enhancing nucleation and impeding growth is seen in the present work in the high density of independent nucleation events on the TiB_2 particles. It is remarkable that even with the high undercoolings there was no nucleation on the non-basal facets of TiB_2.

Overall, when considering the nucleation mechanism rather than subsequent growth, it appears that the crystallization in the metallic glass is a successful analogue of conventional solidification.

Conclusions

In an Al-based metallic glass with added conventional grain refiner (Al – 5 wt.%Ti – 1 wt.%B), TiB_2 particles embedded in the glassy matrix act as centres for subsequent nucleation of α-Al. There are no discrete Al_3Ti particles but the phase does exist as a thin coating on the TiB_2 particles. There is no evidence for survival of Al_3Ti within protective shells of boride particles or within cavities in the boride. Varying the composition of the glassy matrix shows that formation of the Al_3Ti layer and nucleation of α-Al are promoted by the presence of excess Ti (beyond TiB_2) or of other elements, such as Ta, which can form an Al_3X phase isomorphous with Al_3Ti. There are well defined orientation relationships between the TiB_2, Al_3Ti and α-Al in which the close-packed planes and directions are parallel. The observations in the metallic glass, in particular the role of excess Ti and the crystallographic relationship between TiB_2 and α-Al, parallel those in grain-refining in conventional solidification of dilute Al-melts. The experiments in the metallic glass show

clearly, however, that the Al_3Ti (which is a potent nucleant because of its peritectic reaction with α-Al) exists only as a coating on TiB_2 and that nucleation of α-Al (even at high undercooling) is only on the {0001}faces of TiB_2. The lack of nucleation on other faces suggest that re-entrant corners and cavities in boride particles would not be favoured sites. Both chemical and crystallographic effects are important in the nucleation mechanism on refining particles. The nucleation stage of crystallization of α-Al on TiB_2 particles in a glass is a useful slow motion analogue of the action of grain refiners in conventional casting of dilute Al melts and can elucidate significant features of the mechanism. Many questions on grain refinement remain open, particularly on the mechanism of formation or preservation of the Al_3Ti layer and possible influences of solute in the aluminide layer on the nucleation mechanism for α-Al.

Acknowledgements

This work is supported by Alcan International Ltd (Banbury Laboratory) and by London & Scandinavian Metallurgical Co. Ltd. The authors thank Dr M.A. Kearns for a critical reading of the manuscript.

References

[1] M.E.J. Birch and A.J.J. Cowell, "Grain Refinement of Aluminium Alloys Containing Chromium and Zirconium", Solidification Processing 1987, eds J. Becht and H. Jones (London, UK: The Institute of Metals, 1988), 149 – 152.

[2] M.E.J. Birch and P. Fisher, "Mechanism of Fade in Grain Refining of Aluminium with Titanium Boron Aluminium", Solidification Processing 1987, eds J. Becht and H. Jones (London, UK: The Institute of Metals, 1988), 500 – 502.

[3] L. Arnberg, L. Bäckerud and H. Klang, "Possible Grain Refining Mechanisms in Aluminium as a Result of Addition of Master Alloys of the Al-Ti-B type", Grain refinement in Castings and Welds, ed. G.J. Abbaschian and S.A. David, (Warrendale, PA: AIME, 1983), 165 – 181.

[4] T.W. Clyne and M.H. Robert, "Stability of intermetallic Aluminides in Liquid Aluminium and Implications for grain refinement", Metals Techn., 7 (1980), 177 – 185.

[5] A. Cibula, "The Mechanism of Grain Refinement of Sand Castings in Aluminium Aluminium Alloys", J. Inst. Metals, 76 (1949), 323 – 360.

[6] L. Bäckerud, P. Gustafson and M. Johnson, "Grain Refining Mechanism in Aluminium as a Result of Additions of Titanium and Boron: Part II", Aluminium, 67 (1991), 910 – 915.

[7] M. Vader and J. Noordegraaf, "The Effectiveness of a Grain Refiner Reinforced by a Built-in Energy Content", Light Metals 1990, ed.: C.M. Bickert (Warrendale, PA: The Minerals, Metals and Materials Society, 1990), 851 – 857.

[8] D. Turnbull, "Kinetics of Heterogeneous Nucleation", J. Chem. Phys., 18 (1950), 198 – 203.

[9] G. P. Jones, " New Ideas on the Mechanism of Heterogeneous Nucleation in Liquid Aluminium" (NPL Report, DMA (A) 19, National Physical Laboratory, Teddington, U.K., 1983).

[10] D. Turnbull and B. Vonnegut, "Nucleation Catalysis", Ind. Eng. Chem., 44 (1952), 1292 – 1298.

[11] K.F. Kelton, "Crystal Nucleation in Liquids and Glasses", Solid State Physics, 45 (1991), 75 – 177.

[12] P. Schumacher, "Nucleation in Aluminium Alloys Studied Using Devitrification" (Ph.D. thesis, University of Cambridge, U.K., 1994), 82 – 89.

[13] P. Schumacher and A.L. Greer, "Heterogeneously Nucleated α-Al in Amorphous Aluminium Alloys", Mater. Sci. Eng., A178 (1994), 309 – 313.

[14] P. Schumacher and A.L. Greer, "Enhanced Heterogeneous Nucleation of α-Al in Amorphous Aluminium Alloys", Mater. Sci. Eng., A181/A182 (1994), 1335– 1339.

[15] A. Inoue, N. Matsumoto and T. Masumoto, "Al-Ni-Y-Co Amorphous Aluminium Alloys with High Mechanical Strength, Wide Supercooled Liquid Region and Large Glass-Forming Capacity", Mater. Trans. JIM, 6 (1990), 493 – 500.

[16] P. Schumacher and A.L. Greer, "Devitrification of the Stable Al-rich Amorphous Alloy $Al_{85}Y_8Ni_5Co_2$", Key Eng. Mater., 81-83 (1993), 631 – 636.

[17] M. Johnson and L. Bäckerud, "Nucleants in Grain Refined Aluminium after Addition of Ti- and B-containing Master Alloys", Z. Metallkd., 83 (1992), 774 – 780.

[18] P. Schumacher and A.L. Greer, "Nucleation of α-Al on Grain-Refining Particles Studied in Crystallization of Amorphous Al-Alloys", (Proc. 4th International Conference on Aluminum Alloys, Atlanta, Georgia, 11 – 16 August 1994), 730 – 737.

[19] W.T. Kim et al., "TEM Characterisation of Melt Spun Al-3Ti-1B and Al-5Ti-1B Alloys", Int. J. Rapid Solid., 7 (1992), 245 – 254.

[20] L. Arnberg, L. Bäckerud and H. Klang, "Intermetallic Particles in Al-Ti-B-type Master Alloys for Grain Refinement of Aluminium: Part II", Metals Techn., 7 (1982), 7 – 13.

[21] S. Hashimoto, K.F. Kobayashi and S. Miura, "Roles of Lattice Coherency to the Heterogeneous Nucleation in the Al-Ti system", Z. Metallkd., 75 (1983), 787 – 792.

[22] P.S. Mohanty, F.H. Samuel, J.E. Gruzleski and T.J. Kosto, "Studies on the Mechanism of Grain Refinement in Aluminium", Light Metals 1994, ed.: U. Mannweiler (Warrendale, PA: The Minerals, Metals & Materials Society, 1994), 1039 – 1045.